



High-yield production of a super-soluble miniature spidroin for biomimetic high-performance materials

Benjamin Schmuck¹, Gabriele Greco^{2,3}, Andreas Barth⁴, Nicola M. Pugno^{2,5}, Jan Johansson¹, Anna Rising^{1,3,*}

¹ Department of Biosciences and Nutrition, Karolinska Institutet, Neo, 141 86 Huddinge, Sweden

² Laboratory for Bioinspired, Bionic, Nano, Meta, Materials & Mechanics, Department of Civil, Environmental and Mechanical Engineering, University of Trento, Via Mesiano, 77, 38123 Trento, Italy

³ Department of Anatomy, Physiology and Biochemistry, Swedish University of Agricultural Sciences, Uppsala, Sweden

⁴ Department of Biochemistry and Biophysics, Svante Arrhenius väg 16C, Stockholm University, 10691 Stockholm, Sweden

⁵ School of Engineering and Materials Science, Queen Mary University of London, Mile End Road, London E1 4NS, United Kingdom

The mechanical properties of artificial spider silks are approaching a stage where commercial applications become realistic. However, the yields of recombinant silk proteins that can be used to produce fibers with good mechanical properties are typically very low and many purification and spinning protocols still require the use of urea, hexafluoroisopropanol, and/or methanol. Thus, improved production and spinning methods with a minimal environmental impact are needed. We have previously developed a miniature spider silk protein that is characterized by high solubility in aqueous buffers and spinnability in biomimetic set-ups. In this study, we developed a production protocol that resulted in an expression level of >20 g target protein per liter in an *Escherichia coli* fed-batch culture, and subsequent purification under native conditions yielded 14.5 g/l. This corresponds to a nearly six-fold increase in expression levels, and a 10-fold increase in yield after purification compared to reports for recombinant spider silk proteins. Biomimetic spinning using only aqueous buffers resulted in fibers with a toughness modulus of 74 MJ/m³, which is the highest reported for biomimetically as-spun artificial silk fibers. Thus, the process described herein represents a milestone for the economic production of biomimetic silk fibers for industrial applications.

Keywords: Artificial spider silk; Spidroins; Bioreactor cultivation; Recombinant protein expression

Introduction

The favorable mechanical properties (high strength, yet extensible) and the biocompatible and biodegradable nature [1–4] of spider silk have triggered a quest to harness this material for various industrial applications. Unfortunately, the production of native silk is not feasible on large scale due to the territorial and cannibalistic behavior of spiders [5]. Hence, there is a need for economically feasible large-scale production methods of spider silk

proteins (spidroins) using heterologous hosts [6]. Recently, Edlund and co-workers have shown that an economically viable production method using an *Escherichia coli* (*E. coli*) fermentation process and immobilized metal affinity chromatography for protein purification would require an expression level of 10 g/l, enabling a sale price of 23\$/kg for artificial spider silk [7].

Spidroins are large proteins (250–350 kDa) and consist of three distinct domains [8]. The poly-alanine/glycine-rich repeat region is embedded between the N-terminal (NT) [9] and the C-terminal (CT) domains [10], both of which respond with

* Corresponding author.

E-mail address: Rising, A. (anna.rising@ki.se)

conformational changes to a pH gradient along the spiders spinning duct [10–13]. This pH dependency of NT and CT together with shear forces trigger the assembly of the spidroins into mature silk fibers.

The presence of the highly repetitive region between NT and CT, containing up to a hundred tandem repeats, makes a high-yield recombinant expression of native spidroins difficult to achieve [14,15] due to limitations of the translation machinery of bacterial hosts [16–18]. To attenuate these constraints codon optimization and upregulating ^{glycyl}tRNA are suggested as effective countermeasures [14,18–21]. Applying this strategy for expressing spidroins in *E. coli* resulted in the highest expression level reported thus far using a bioreactor (3.6 g/l, Table 1), though it should be noted that this is before protein purification and does not reflect the final yield. In addition to the relatively low yields, the recombinant spidroins are prone to aggregate, which is why common techniques to prepare the spinning solutions (dopes) include the use of denaturing agents like urea/guanidium for the re-suspension of inclusion bodies, hexafluoroisopropanol (HFIP) for solubilizing lyophilized proteins, and methanol/isopropanol as a coagulation agent for spinning [14,19,22,23]. Fibers produced using these methods have reached the toughness modulus of native spider silk, provided that additional manual post-spin stretching is applied [14,19,22]. Nevertheless, these harsh conditions are very different from the conditions spiders use to make silk [13,24] and leave the process expensive and harmful to the environment [7,25].

To push the yield to the economically viable level of 10 g/l, we speculated that the designed mini-spidroin NT2RepCT (two natural tandem repeat units flanked by the terminal domains) known for its high solubility of up to 500 mg/ml in aqueous buffers and proper response to lowered pH in biomimetic spinning set-ups [26–29] (Fig. 1a–c), is a suitable candidate for expression in a high-cell density culture. In support of this, bacterial shake-flask cultivations employing the standard *E. coli* BL21 (DE3) strain express NT2RepCT with a yield in a range above 100 mg/l [26], which is a good starting point for further optimizations.

Results and discussion

Our initial attempt to produce NT2RepCT in a high-cell density culture (batch 150I) relied on our previous expression protocols for shake-flasks [26] and a semi-defined cultivation medium with glycerol as the main carbon source suggested by da Silva and co-

workers [30]. Thus, compared to the shake-flask protocol we implemented several adjustments for the expression of NT2RepCT in the bioreactor. First, instead of LB-medium, we used a complex growth medium combined with trace metals, phosphate buffer, and an additional carbon source (glucose and glycerol). Second, protein expression was first induced when the optical density at 600 nm (OD₆₀₀) was >50, instead of around 1. Third, to enable continued growth we implemented a fed-batch setup, with glycerol as the main feed [31].

Briefly, the culture was grown at 25 °C, before the temperature was decreased to 20 °C when OD₆₀₀ reached 50, and protein expression was induced with IPTG (150 μM). Feeding with 40% glycerol started automatically once the initial carbon source (a combination of glycerol and glucose) was depleted (see Fig. S1 for the cultivation plots). After ~30 h pO₂ suddenly spikes, indicating that the depletion of the carbon source. When using this protocol, 22 h after induction NT2RepCT reached an expression level of 13.2 g/l in batch 150I.

Next, we wanted to investigate if moderately higher IPTG concentration for induction would increase the protein yield, and likewise monitor how NT2RepCT accumulates after induction (Fig. 2). To reduce the stress on the culture and enable continued growth [32,33], we decided not to apply higher IPTG concentrations than 250 μM. Independent of the IPTG concentration used for inducing protein expression (150, 200, or 250 μM, named batch 150I_2, 200I, and 250I, respectively), 20 h after induction a plateau is reached with respect to the protein yield (Fig. 2b). The highest NT2RepCT expression level was obtained with 250 μM IPTG, which gave 15.9 g/l (Fig. S2). However, a correlation between the expression level and the IPTG concentration in the tested range could not be observed (Fig. 2b), which means that the differences are most likely attributed to experimental batch-to-batch variations rather than differences in IPTG concentrations (compare also batch 150I and 150I_2, Table S1).

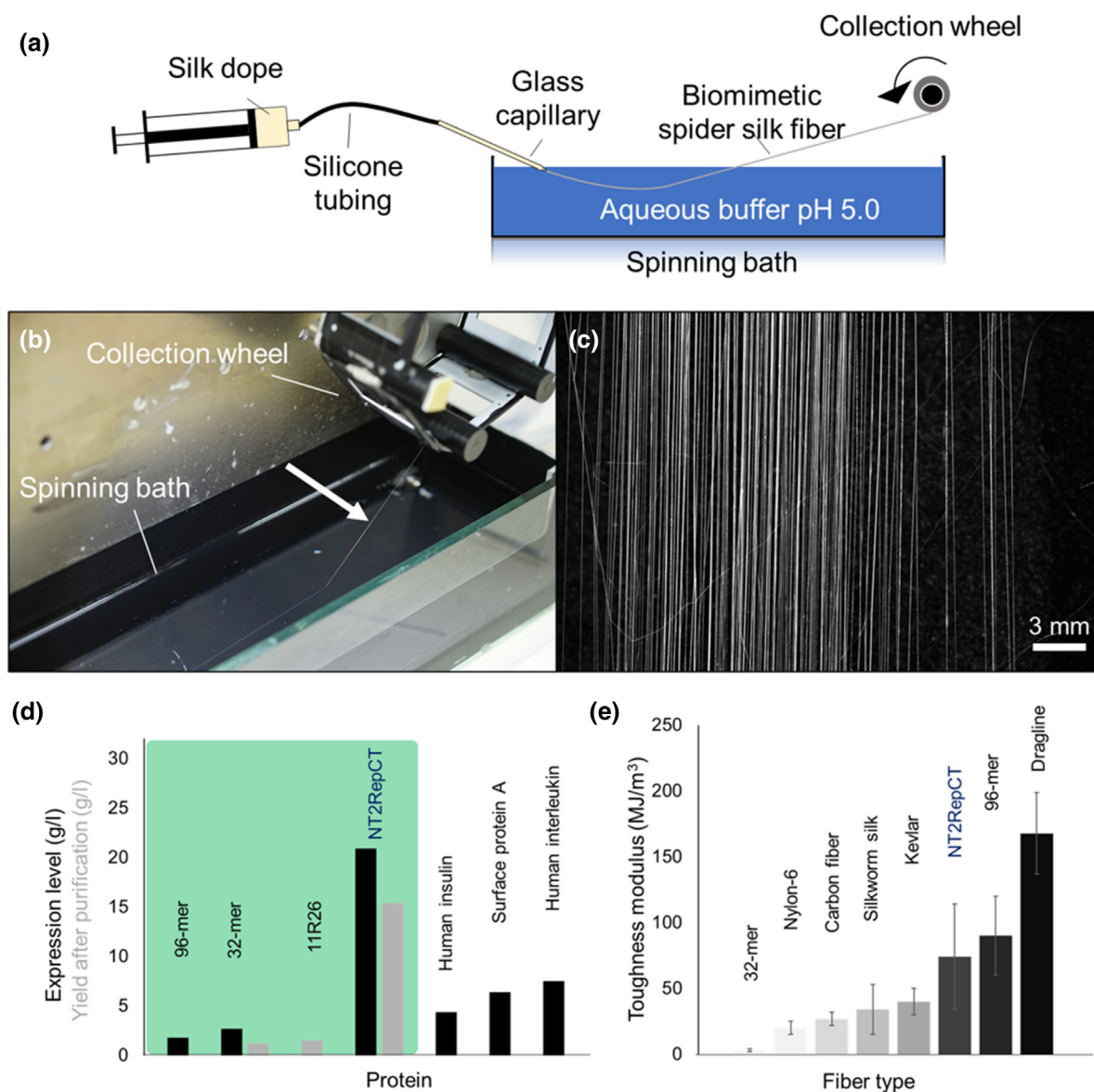
Finally, the cultivation of *E. coli* expressing NT2RepCT was repeated once more but using a larger reactor vessel (final cultivation volume 1.6 l, batch 150IL). Since IPTG can be toxic to the cells [34] and since we did not observe an improved final protein yield when using higher IPTG concentrations (Table S1), we chose to continue to induce the cultures with 150 μM IPTG. Initially, the bacteria were allowed to grow at 29 °C to OD₆₀₀ of 77, before reducing the temperature to 20 °C for induction. 21 h after induction, the culture accumulated an impressive 20.9 g/l of NT2RepCT (estimated with SDS PAGE Table 1, Fig. 1d, and

TABLE 1

Spidroin expression with *E. coli* using a bioreactor.

Culture size (l)	Spidroin ^a	Expression level (g/l)	Yield after purification (g/l)	Size (kDa)	Solubility after expression	Solvent ^b	Reference
2–5	11R26	n.r.	1.5	18	6 M urea	HFIP	[20]
2	96-mer	1.8	n.r.	290	8 M urea	HFIP	[19]
2	32-mer	2.7	1.2	100	8 M urea and 2 M thiourea	HFIP	[14]
~2	MaSp2	3.6	n.r.	202	buffer ^c	n.a. ^d	[21]
1.6	NT2RepCT	20.9	14.5	33	20 mM Tris, pH 8	n.a.	this study

n.r. – not reported. n.a. – not applicable. a) The spidroin names reported in this table correspond to names reported in the listed references. For instance, “32-mer” means that the spidroin contains 32 tandem repeat units of poly-alanine/glycine-rich regions. MaSp 2 contains 64 iterated consensus repeats and the minispidroin NT2RepCT has 2 tandem repeat units and both terminal domains. b) Solvent used to resolubilize lyophilized artificial spidroins after purification. c) The composition of the buffer is not reported. d) The MaSp2 expressed in this study was not purified, and not used for spinning artificial silk.

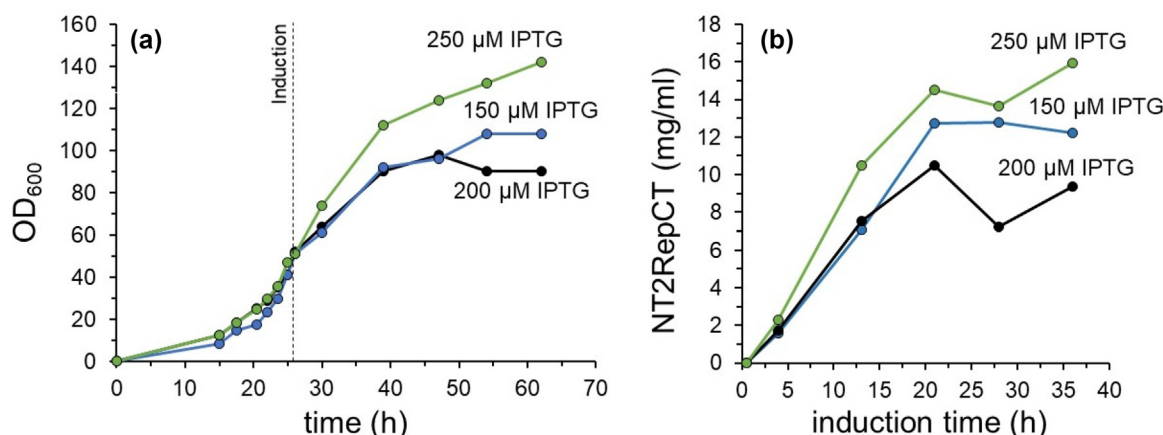
**FIGURE 1**

Biomimetic spinning setup used to spin the minispidroin NT2RepCT, and comparison of the expression level, yield after purification, as well as the toughness modulus of produced artificial silk with reference proteins/materials. (a) Schematic image of biomimetic spinning: A concentrated solution of NT2RepCT (dope; protein concentration 300 mg/ml in mild aqueous buffer, pH 8) is extruded through a glass capillary into a spinning bath containing an aqueous buffer, pH 5. The pH change and shear forces mimic the conditions of native silk spinning and induce immediate fiber formation. (b, c) The fibers are collected continuously on a collection wheel with a speed of 46 cm s⁻¹ (See also [Supplementary Video 1](#)). (d) Comparison of the expression level and yield after purification of artificial spidroins (highlighted in green) that were previously expressed using *E. coli* in bioreactor cultivations (96-mer see Ref. [19], 32-mer see Ref. [14], silk protein 11R26 see Ref. [20], and more details in [Table 1](#)). As a reference, the graph also includes the highest (to the best of our knowledge) reported expression yields using *E. coli* for human insulin [47], human interleukin-6 [48], and surface protein A (SpaA) from *Erysipelothrix rhusiopathiae* [30]. (e) The toughness modulus of NT2RepCT fibers (this study) compared to fibers from artificial spidroins 96-mer and 32-mer [14,19]; synthetic fibers Nylon 6 [49], Kevlar (see method section in Supporting Information), and Carbon fibers (see method section in Supporting Information); silkworm silk [50], and native dragline spider silk [4].

Fig. S3. The expression level was also estimated considering the dry cell weight to 20.8 g/l. See [Fig. S4](#) and [Table S1](#)). A summary of the cultivation parameters and yields is found in [Table S1](#).

The improved cultivation conditions in combination with the relatively small size (33 kDa) and the high solubility of NT2RepCT are likely reasons for the high expression level after culture harvest. Of note, the high solubility of NT has been exploited to develop a tool for the production of aggregation-

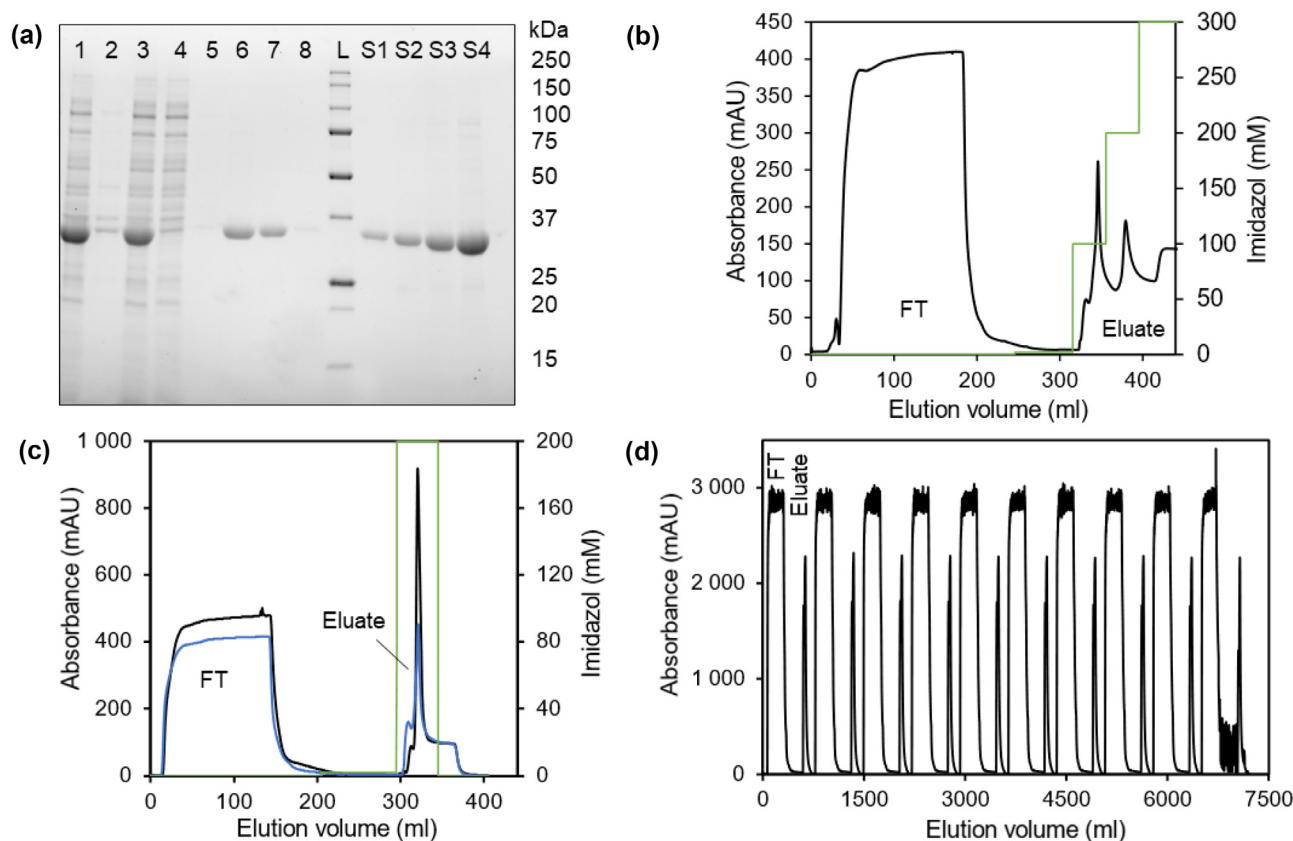
prone proteins at large [35–39] and could contribute to high yield and solubility also for NT2RepCT. The resulting 20.9 g/l is nearly a 6-fold increase compared to previous bioreactor cultivations of spidroins [14,19,20,21], and twice the level that has been judged economical for commercialization of recombinant silk-based products [7]. In fact, this is among the highest protein expression levels reported to date for *E. coli* produced proteins [30,40–42].

**FIGURE 2**

Expression of NT2RepCT in *E. coli* in a high-cell density culture (0.35 l) using different IPTG concentrations. (a) OD₆₀₀ of the *E. coli* culture over time before and after induction. The induction point is indicated by the dashed line. (b) The concentration of NT2RepCT in the culture was estimated with SDS-PAGE as a function of induction time.

The downstream processing required no denaturing agents or organic solvents, which makes the entire procedure sustainable and environmentally friendly. After cell lysis using a 20 mM Tris-HCl buffer at pH 8, an insignificant amount of NT2RepCT

remained in the pellet after centrifugation (Fig. 3a), and ~95% of NT2RepCT was present in the cell lysate. The target proteins bound efficiently to the columns and the minimum concentration of imidazole required to elute NT2RepCT was investigated

**FIGURE 3**

Purification of NT2RepCT expressed in the bioreactor using IMAC. (a) SDS-PAGE of lane 1: Total cell content (2-fold dilution); 2: pellet after centrifugation (2-fold dilution); 3: lysate (2-fold dilution); 4: flow-through (2-fold dilution); 5: wash 5 mM imidazole; 6: 100 mM imidazole (10-fold dilution); 7: 200 mM imidazole (10-fold dilution); 8: 300 mM imidazole; L: Ladder. S1–S4 reference samples of NT2RepCT. S1: 0.225 mg/ml; S2: 0.45 mg/ml; S3: 0.9 mg/ml; S4: 1.8 mg/ml. (b) Step elution of protein (black line) from a 20 ml HisPrep FF 16/10 with 100-, 200-, and 300-mM imidazole (green line). (c) Purification of NT2RepCT (batch 250l) with 20 ml HisPrep FF 16/10 (blue line) or HiTrap Chelating HP four-time 5 ml sequentially coupled columns (black line). (d) Processing large quantities of lysate, by using a fully automated protocol for repeated loading and elution (batch: 150l).

by using a step gradient, which included 100-, 200-, and 300-mM imidazole (Fig. 3b). While most NT2RepCT eluted with 100 mM imidazole, elution with 200 mM was essential to maximize the yield. Next, we compared the purification of NT2RepCT with either 4x5ml HiTrap Chelating HP sequentially coupled columns or a 20 ml HisPrep FF 16/10 column to test if the choice of the column influenced the yield (Fig. 3c). The yield using the HiTrap column was estimated to 11.2 g/l, which is indistinguishable from 11.4 g/l, estimated with the HisPrep column.

Since the columns have a theoretical maximal binding capacity of only 500–800 mg/20 ml medium, we had to establish an automated protocol for repeated loading of lysate and elution of protein to purify more than just a fraction of each batch (Fig. 3d, see SDS-PAGE gel image of the purification in Fig. S5). This made storage of the eluate for longer periods in the cold (6 °C up to 24 h) indispensable. Unexpectedly, the eluate indeed remained clear, and no protein aggregation was observed during the storage of the centrifugated lysate. By using the automated purification procedure, 14.5 g/l NT2RepCT was obtained from batch 150IL, which is 10 times higher than previously reported for recombinant spidroins (Table 1, Fig. 1d). Independent of the batch, purification recovered approximately 70% of the total expressed protein. Thus, the herein achieved production levels and yields after purification, as well as the protein solubility and stability during expression and purification, are unprecedented when comparing to previously published spidroin production protocols (Table 1, Fig. 1d).

Biomimetic spinning was performed using a custom-made device that extruded a concentrated NT2RepCT solution (dope) with a pump-driven syringe through a pulled glass capillary into an aqueous buffer (500 mM Na-acetate, 200 mM NaCl, pH 5) (Fig. 1a–c) [26]. The silk formed immediately once the dope entered the spinning buffer and was collected in air on a rotating wheel placed at the end of the 80 cm long bath. This spinning process is continuous (Supplementary Video 1) and was carried out for several minutes but could in principle be extended to several hours. From one bioreactor culture (1.6 l), 23 g of pure NT2RepCT was obtained, which is enough to prepare 77 ml dope (300 mg/ml). Considering the flow rate for spinning (17 μ l/min) and a reeling speed of 46 cm s⁻¹, this amount is enough to spin continuously for 75 h, which corresponds to a 125 km long fiber.

A closer investigation revealed that fibers made from NT2RepCT produced in the bioreactor (batch 150I, 250I, and 150IL) had diameters of <12 μ m and the morphology was similar to previously reported fibers made from NT2RepCT produced in shake flasks [26,43,44]. SEM revealed that the fibers are smooth from one side and possess a longitudinal groove along the other side. Under a light microscope, they appeared as straight, twisted, or exhibited a longitudinal groove (Fig. 4 and Fig. S6 for representative micrographs), which are common morphologies of synthetic artificial silk fibers [19,45].

A potential problem for commercial applications of artificial silk fibers is the inherent variability in mechanical properties, which can be observed even for fibers that are spun from the

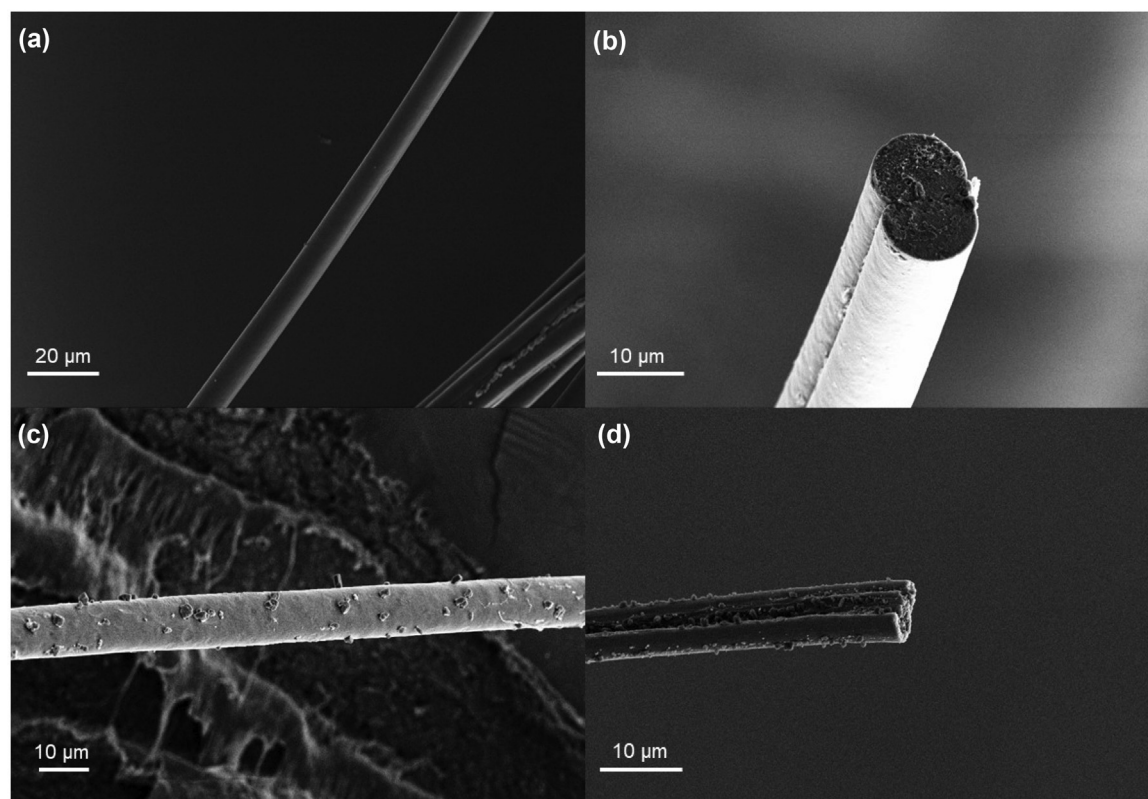


FIGURE 4

Representative SEM images show uniform fibers with a smooth surface on one side and a longitudinal groove on the other side. (a and b) Representative images of fibers which were spun using NT2RepCT from batch 150I. (c and d) Representative images of fibers spun with NT2RepCT from batch 250I.

TABLE 2

Mechanical properties of biomimetic silk fibers from NT2RepCT expressed in the bioreactor.

Batch	Diameter (μm)	Strain at break (%)	Toughness modulus (MJ m^{-3})	Strength (MPa)	Young's modulus (GPa)
150I	11.5 ± 2.1	$94\% \pm 36\%$	74 ± 40	99 ± 29	2.5 ± 0.7
250I	8.1 ± 2.6	$86\% \pm 29\%$	70 ± 35	101 ± 30	2.8 ± 0.9
150IL	7.0 ± 1.2	$87\% \pm 17\%$	64 ± 16	95 ± 20	2.2 ± 0.6

20 fibers were tested for each set. Outliers were not removed.

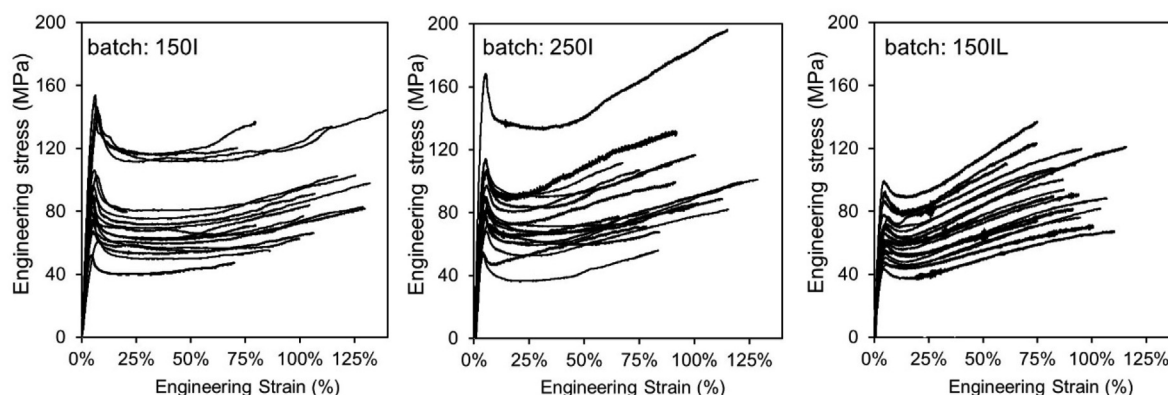


FIGURE 5

Stress-strain curves of NT2RepCT fibers produced in this study. For each set of fibers, 20 randomly selected fibers were tested. Outliers were not removed. The data shown were smoothed to reduce the noise with a moving average function in Microsoft Excel®.

same recombinant protein [26,27,43,44]. The most likely explanation for these variations are subtle differences in the spinning methods used in the respective studies, e.g., size and shape of the capillary nozzle, speed of fiber collection, and time the fiber spends in the bath before being collected in air. Thus, we spun fibers from batch 150I, 250I, and 150IL paying meticulous attention to provide identical spinning conditions. NT2RepCT was spun using a dope extrusion speed of $17 \mu\text{l}/\text{min}$, a capillary opening diameter of $35 \pm 5 \mu\text{m}$, and 80 rpm collection wheel speed (46 cm s^{-1} silk fiber collection speed) with the wheel positioned at the end of the 80 cm long bath. Our results show that NT2RepCT produced from three different batches, purified with different columns, and spun at different occasions exhibit mechanical properties that are indistinguishable from each other. The fibers are very extensible (strain at break $\sim 90\%$), have a significant strength of around 100 MPa, a Young's modulus of $\sim 2.7 \text{ GPa}$, and a toughness modulus of 70 MJ m^{-3} (Table 2 and Fig. 5). The average toughness modulus value between the batches varied by less than $\pm 8\%$. Also, the Fourier Transform Infrared (FTIR) spectra (Fig. 6 and Fig. S7) of fibers from batch 150I and 250I are very similar in the amide I region and showed that the β -sheet content in both samples is $\sim 40\%$.

The fibers produced using the herein described method have higher strength and toughness modulus compared to previously described as-spun (without post-spin stretching) artificial silk fibers [26,27,43]. Compared to native dragline silk, the toughness modulus of NT2RepCT fibers is around 50%, and compared to artificial silk fibers that have been produced from recombinant spidroins with reported expression levels $>1.5 \text{ g/l}$, the toughness modulus is equal or significantly higher (Fig. 1e). The large protein yields and practically feasible spinning method are impor-

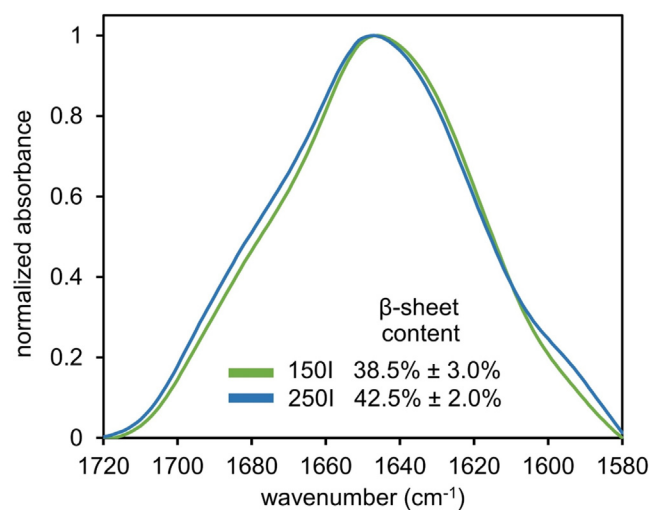


FIGURE 6

FTIR spectra of fibers from NT2RepCT (batch 150I and 250I), in the amide I region ($1700\text{--}1600 \text{ cm}^{-1}$). The spectra were baseline subtracted and normalized. A detailed description of the secondary structure analysis is provided in the SI and illustrated in Fig. S7.

tant stepping-stones for further improving the fiber properties, e.g. by protein engineering approaches [46].

Concluding remarks

This study describes a protocol for expressing NT2RepCT with an *E. coli* fed-batch culture that yields more than 14 g/l of pure protein. The protocol is surprisingly simple: a standard *E. coli* strain and expression vector was used together with an optimized

cultivation medium composition but without the need of upregulating ^{glycyl}tRNA. In the race to make the production of artificial spider silk economically feasible, this is an important step forward. According to a previously published study the expression levels of artificial spider silk proteins must reach 10 g/l to enable a sale price of 23\$/kg for artificial spider silk fibers [7]. The process used for the cost estimation was similar to our method in the expression and down-stream purification parts, but included the use of organic solvents for fiber spinning. The high spidroin expression level reported herein (~20 g/l) combined with the use of solely aqueous buffers for fiber spinning vouch for economically feasible production costs.

Furthermore, the biomimetic spinning setup reported in this study resulted in fibers with reproducible mechanical properties, exhibiting a higher toughness modulus and strength than any previously reported as-spun biomimetic spider silk fiber.

Materials and methods

A detailed description of the methodology used in this study including all references are described in the [Supplementary information](#), available online. There, a description of how the bioreactor cultivations were carried out, the exact purification protocol, the biomimetic spinning procedure, and fiber characterization techniques are found.

Funding details

This work was supported by European Research Council (ERC) under the European Union's Horizon 2020 research and innovation program (grant agreement No 815357), the Center for Innovative Medicine (CIMED) at Karolinska Institutet and Stockholm City Council, Karolinska Institutet SFO Regen (FOR 4-1364/2019), the Swedish Research Council (2019-01257), Olle Engkvist stiftelse (207-0375), and Formas (2019-00427). N. M. P. is supported by the European Commission under the FET Proactive ("Neurofibers") grant No. 732344 as well as by the Italian Ministry of Education, University and Research (MIUR) under the "Departments of Excellence" grant I. 232/2016, the ARS01-01384-PROSCAN and the PRIN-20177TTP3S grants. G. G. is supported by Caritro Foundation (prot. U1277.2020/SG.1130), and by Olle Engkvist stiftelse.

CRediT authorship contribution statement

Benjamin Schmuck: Conceptualization, Methodology, Validation, Investigation, Writing – original draft, Writing - review & editing, Visualization. **Gabriele Greco:** Validation, Investigation, Writing - review & editing, Visualization. **Andreas Barth:** Validation, Resources, Writing - review & editing. **Nicola M. Pugno:** Writing - review & editing, Funding acquisition, Resources. **Jan Johansson:** Writing - review & editing, Supervision, Funding acquisition, Resources. **Anna Rising:** Conceptualization, Methodology, Writing - review & editing, Supervision, Funding acquisition, Resources.

Declaration of Competing Interest

The authors declare that they have no known competing financial interests or personal relationships that could have appeared to influence the work reported in this paper.

Acknowledgements

The authors thank Mats Sandgren, who provided the bioreactor infrastructure located at the Biocentrum, Swedish University of Agricultural Sciences, Uppsala, Sweden. The authors would like to thank Lorenzo Moschini, Prof. Antonella Motta, and Prof. Claudio Migliaresi (Biotech – Mattarello, University of Trento) for their support with the SEM facility.

Declaration of competing interest

No potential conflict of interest was reported by the author(s).

Data availability

The raw data of the results presented in this study are available through the corresponding author on reasonable request.

Appendix A. Supplementary data

Supplementary data to this article can be found online at <https://doi.org/10.1016/j.mattod.2021.07.020>.

References

- [1] C. Radtke et al., PLoS One 6 (2011) e16990, <https://doi.org/10.1371/journal.pone.0016990>.
- [2] C. Allmeling et al., Cell Prolif. 41 (2008) 408–420, <https://doi.org/10.1111/j.1365-2184.2008.00534.x>.
- [3] I. Agnarsson, M. Kuntner, T.A. Blackledge, C. Lalueza-Fox, PLoS One 5 (2010) e11234, <https://doi.org/10.1371/journal.pone.0011234>.
- [4] G. Greco, N.M. Pugno, Molecules 25 (2020) 2938, <https://doi.org/10.3390/molecules25122938>.
- [5] D.H. Wise, Annu. Rev. Entomol. 51 (2006) 441–465, <https://doi.org/10.1146/annurev.ento.51.110104.150947>.
- [6] G. Bhattacharyya et al., Protein Expr. Purif. 183 (2021) 105839, <https://doi.org/10.1016/j.pep.2021.105839>.
- [7] A.M. Edlund et al., N. Biotechnol. 42 (2018) 12–18, <https://doi.org/10.1016/j.nbt.2017.12.006>.
- [8] N.A. Ayoub et al., PLoS One 2 (2007) e514, <https://doi.org/10.1371/journal.pone.0000514>.
- [9] A. Rising et al., Biomacromolecules 7 (2006) 3120–3124, <https://doi.org/10.1021/bm060693x>.
- [10] F. Hagn et al., Nature 465 (2010) 239–242, <https://doi.org/10.1038/nature08936>.
- [11] G. Askarieh et al., Nature 465 (2010) 236–238, <https://doi.org/10.1038/nature08962>.
- [12] N. Kronqvist et al., Nat. Commun. 5 (2014) 3254, <https://doi.org/10.1038/ncomms4254>.
- [13] M. Andersson et al., PLoS Biol. 12 (2014), <https://doi.org/10.1371/journal.pbio.1001921>.
- [14] X.X. Xia et al., Proc. Natl. Acad. Sci. U. S. A. 107 (2010) 14059–14063, <https://doi.org/10.1073/pnas.1003366107>.
- [15] A. Rising et al., Cell. Mol. Life Sci. 68 (2011) 169–184, <https://doi.org/10.1007/s00018-010-0462-z>.
- [16] V.G. Debabov, V.G. Bogush, ACS Biomater. Sci. Eng. 6 (2020) 3745–3761, <https://doi.org/10.1021/acsbiomaterials.0c00109>.
- [17] M.B. Hinman, J.A. Jones, R.V. Lewis, Trends Biotechnol. 18 (2000) 374–379, [https://doi.org/10.1016/S0167-7799\(00\)01481-5](https://doi.org/10.1016/S0167-7799(00)01481-5).
- [18] S.R. Fahnestock, S.L. Irwin, Appl. Microbiol. Biotechnol. 47 (1997) 23–32, <https://doi.org/10.1007/s002530050883>.
- [19] C.H. Bowen et al., Biomacromolecules 19 (2018) 3853–3860, <https://doi.org/10.1021/acs.biomac.8b00980>.
- [20] H. Zhang et al., Prep. Biochem. Biotechnol. 46 (2016) 552–558, <https://doi.org/10.1080/10826068.2015.1084637>.
- [21] Y.X. Yang et al., Process Biochem. 51 (2016) 484–490, <https://doi.org/10.1016/j.procbio.2016.01.006>.
- [22] A. Heidebrecht et al., Adv. Mater. 27 (2015) 2189–2194, <https://doi.org/10.1002/adma.201404234>.
- [23] A. Koeppel, C. Holland, ACS Biomater. Sci. Eng. 3 (2017) 226–237, <https://doi.org/10.1021/acsbiomaterials.6b00669>.

- [24] A. Rising, J. Johansson, *Nat. Chem. Biol.* 11 (2015) 309–315, <https://doi.org/10.1038/nchembio.1789>.
- [25] J.J. Milne, Scale-up of protein purification: Downstream processing issues, *Methods Mol. Biol.*, 2017: 71–84, https://doi.org/10.1007/978-1-4939-6412-3_5.
- [26] M. Andersson et al., *Nat. Chem. Biol.* 13 (2017) 262–264, <https://doi.org/10.1038/nchembio.2269>.
- [27] N. Gonska et al., *Biomacromolecules* 21 (2020) 2116–2124, <https://doi.org/10.1021/acs.biomac.0c00100>.
- [28] M. Landreh et al., *Chem. Commun.* 53 (2017) 3319–3322, <https://doi.org/10.1039/C7CC00307B>.
- [29] M. Otikovs et al., *Angew. Chem. Int. Ed.* 56 (2017) 12571–12575, <https://doi.org/10.1002/anie.201706649>.
- [30] A.J. da Silva et al., *Springerplus* 2 (2013) 1–12, <https://doi.org/10.1186/2193-1801-2-322>.
- [31] M.A. Eiteman, E. Altman, *Trends Biotechnol.* 24 (2006) 530–536, <https://doi.org/10.1016/j.tibtech.2006.09.001>.
- [32] Y. Sevastyanovich et al., *FEMS Microbiol. Lett.* 299 (2009) 86–94, <https://doi.org/10.1111/j.1574-6968.2009.01738.x>.
- [33] C. Wyre, T.W. Overton, *J. Ind. Microbiol. Biotechnol.* 41 (2014) 1391–1404, <https://doi.org/10.1007/s10295-014-1489-1>.
- [34] P. Dvorak et al., *Microb. Cell Fact.* 14 (2015) 201, <https://doi.org/10.1186/s12934-015-0393-3>.
- [35] N. Kronqvist et al., *Nat. Commun.* 8 (2017) 15504, <https://doi.org/10.1038/ncomms15504>.
- [36] A. Abelein et al., *Sci. Rep.* 10 (1) (2020), <https://doi.org/10.1038/s41598-019-57143-x>.
- [37] M. Sarr et al., *FEBS J.* 285 (2018) 1873–1885, <https://doi.org/10.1111/febs.14451>.
- [38] E.H. Abdelkader, G. Otting, *J. Biotechnol.* 325 (2021) 145–151, <https://doi.org/10.1016/j.jbiotec.2020.11.005>.
- [39] G. Chen et al., *Nat. Commun.* 8 (2017) 2081, <https://doi.org/10.1038/s41467-017-02056-4>.
- [40] J.H. Choi, K.C. Keum, S.Y. Lee, *Chem. Eng. Sci.* 61 (2006) 876–885, <https://doi.org/10.1016/j.ces.2005.03.031>.
- [41] M. Merlin et al., *Biomed. Res. Int.* 2014 (2014) 1–14, <https://doi.org/10.1155/2014/136419>.
- [42] J. Kopp et al., *Bioeng. Biotechnol.* 8 (2020) 1312, <https://doi.org/10.3389/fbioe.2020.573607>.
- [43] G. Greco et al., *Molecules* 25 (2020) 3248, <https://doi.org/10.3390/molecules25143248>.
- [44] G. Greco et al., *Commun. Mater.* 2 (2021) 43, <https://doi.org/10.1038/s43246-021-00147-w>.
- [45] F. Müller, S. Zainuddin, T. Scheibel, *Molecules* 25 (2020) 5540, <https://doi.org/10.3390/molecules25235540>.
- [46] J. Johansson, A. Rising, *ACS Nano* 15 (2021) 1952–1959, <https://doi.org/10.1021/acsnano.0c08933>.
- [47] C.S. Shin et al., *Biotechnol. Prog.* 13 (1997) 249–257, <https://doi.org/10.1021/bp970018m>.
- [48] T.W. Kim, B.H. Chung, Y.K. Chang, *Biotechnol. Prog.* 21 (2005) 524–531, <https://doi.org/10.1021/bp049645j>.
- [49] F. Xu et al., *Nanotechnology* 25 (2014) 325701, <https://doi.org/10.1088/0957-4484/25/32/325701>.
- [50] Y. Yang et al., *Mater. Sci. Eng. C* 107 (2020) 110197, <https://doi.org/10.1016/j.msec.2019.110197>.